Pergamon

Int. J. Mech. Sci. Vol. 40, No. 9, pp. 927–936, 1998

Printed in Great Britain
0020–7403/98 $19.00 + 0.00

PII: S0020–7403(97)00146–X

STIFFNESS IDENTIFICATION OF LAMINATED COMPOSITE SHAFTS

T. Y. KAM and C. K. LIU

Mechanical Engineering Department, National Chiao Tung University, Hsin-Chu 30050, Taiwan, R.O.C.

(*Received* 19 *November* 1996; *and in revised form* 12 *November* 1997)

Abstract—Distributions of bending stiffness along the spans of laminated composite shafts are determined via a non-destructive evaluation approach. The finite element method formulated on the assumption of uniform bending stiffness within each element is used in the deflection analysis of the shafts. Differences between measured and theoretically predicted deflections at any two points on a shaft are used to construct an error function for deflection. The identification of bending stiffness is formulated as a minimization problem in which the elemental bending stiffnesses are determined to make the error function a global minimum. A global minimization technique and a bounding method for establishing side constraints are presented to solve the above minimization problem. Experiments are performed to study the feasibility and applications of the proposed method. © 1998 Elsevier Science Ltd. All rights reserved

Keywords: composite materials, finite element method, nondestructive evaluation, beam theory, structural engineering, optimization, experimental technique.

INTRODUCTION

Laminated composite materials have been widely used in the construction of high-performance structures in recent years. To ensure high reliability, the actual behaviors of the laminated composite structures in service must be accurately predicted and carefully monitored. As is well known, there are many methods for manufacturing laminated composite components [1, 2] and different manufacturing or curing processes may yield different mechanical properties of the components. Furthermore, the material properties determined from standard specimens tested in laboratory may deviate significantly from those of actual laminated composite components manufactured in factory. On the other hand, laminated composite structures subject to dynamic loads may experience progressive stiffness reduction which will finally lead to the failure of the structures. It has been pointed out that accurate determination of current stiffness of a laminated composite structure can help prevent sudden failure of the structure [3]. Therefore, the determination of realistic material or mechanical properties of laminated composite components has become an important topic of research. In the past two decades, a number of non-destructive evaluation techniques have been proposed for the determination of material properties of or damages in laminated composite parts [4–7]. Nevertheless, these techniques have their own limitations or specific difficulties when in use. On the other hand, a number of researchers have presented methods to identify or improve the analytical system matrices of a structure using vibration test data [8–13]. For instance, Berman and Nagy [8] developed a method which used measured normal modes and natural frequencies to improve an analytical mass and stiffness matrix model of a structure. Their method could find minimum changes in the analytical model to make it exactly agree with the set of measured modes and frequencies. Kam and Lee [9–11] developed methods to identify the element bending stiffnesses of a damaged structure from which the damages in the structure could be detected using measured natural frequencies and mode shapes.

In this paper, a non-destructive evaluation method is presented for the determination of bending stiffness distribution of laminated composite shafts. The method is based on the minimization of the sum of the differences between predicted and measured deflections at any two points on the shaft. Experiments are carried out to investigate the accuracy and feasibility of the proposed method.

DEFLECTION OF LAMINATED COMPOSITE SHAFTS

Consider a laminated composite shaft composed of laminated composite plies of various fiber angles. The equivalent Young's modulus $E(x)$ and the wall thickness $t(x)$ of the shaft may vary along

the span of the shaft. The deflection of the shaft is analyzed using the finite element method which is formulated on the basis of the simple beam theory. The shaft is divided into a number of elements. The bending stiffness is assumed to be uniform within each element and different elements may have different bending stiffnesses. If the bending stiffness distribution of the shaft is given, the transverse deflection of the shaft can be determined by solving the following load–displacement relation [14]:

$$\mathbf{KU} = \mathbf{F} \tag{1a}$$

or

$$\mathbf{U} = \mathbf{K}^{-1}\mathbf{F}, \tag{1b}$$

where $\mathbf{K}$ is the condensed structural stiffness matrix; $\mathbf{U}$ is the vector of vertical nodal displacements; $\mathbf{F}$ is the condensed vector of nodal forces. It is noted that $\mathbf{K}$ is obtained using the method of static condensation and the terms in $\mathbf{K}$ depend on the bending stiffnesses of the elements. If the elemental bending stiffnesses are not specified, their values can be identified using measured transverse deflection of the shaft via the solution of a minimization problem as will be described in the following section.

DETERMINATION OF BENDING STIFFNESS

It is not uncommon that material properties provided by suppliers or determined from laboratory tests following the standard procedure [15] are used to predict mechanical behaviors of laminated composite structures. The bending stiffness determined from the above material properties is termed as initial bending stiffness $(EI)^{\circ}$ and the deflection so obtained is initial deflection $\mathbf{U}^{\circ}$. Let $(EI)^{*}$ be the actual bending stiffness and $\mathbf{U}^{*}$ the actual deflection. In general, the actual bending stiffness is different from the initial bending stiffness. It can be shown that the actual elemental bending stiffnesses of a shaft can be determined directly from Eqn (1) if all vertical nodal displacements of the shaft are available. For cases where a portion of the vertical nodal displacements are measured, the elemental bending stiffnesses can only be estimated in an indirect way. Herein, the problem of bending stiffness identification is formulated as a minimization problem. In mathematical form it is stated as

$$\begin{aligned} &\text{Min} && \varepsilon(\mathbf{a}^{*}) = (\mathbf{U} - \mathbf{U}^{*})^{t}(\mathbf{U} - \mathbf{U}^{*}) \\ &\text{s.t.} && a_i^L < a_i^{*} < a_i^U, \quad i = 1, \ldots, m, \\ & && a_j^{*} = \bar{a}_j, \qquad\quad i = 1, \ldots, (NE - m), \end{aligned} \tag{2}$$

where $\mathbf{a}^{*} = [(EI)_1^{*}, (EI)_2^{*}, \ldots, (EI)_m^{*}]$; $\mathbf{U}$ is an $N \times 1$ vector containing measured displacements at N specific points on the shaft; ε is an error function measuring the sum of differences between the actual and measured deflections; NE is number of elements; m is the number of parameters to be identified; a_i^L and a_i^U are the lower and upper bounds of $\mathbf{a}_i^{*}$, respectively; $N < m$; $\bar{a}_j$ are the prescribed values of the elemental bending stiffnesses for the elements where no uncertainty exists.

The minimization problem stated above may contain a number of local minima and thus the determination of the global minimum cannot be accomplished by utilizing any local minimizer. Herein a multi-start global minimization algorithm is presented to solve the above problem. Figure 1 shows the flow chart of the minimization algorithm. The random generator *RNUNF* of the *IMSL* mathematical package [16] is used to generate starting points. For each starting point, the minimization routine *BCONF* of the *IMSL* mathematical package is used to solve the above minimization problem for determining the elemental bending stiffnesses $\mathbf{a}^{*}$. The *BCONF* routine can minimize a function of n variables subject to bounds on the variables using a quasi-Newton method and finite difference gradient. The upper and lower bounds of the design variables are properly chosen to ensure the convergence of the solution. A Bayesian argument is used to establish the probability of the current overall minimum value of ε being the global minimum, given the number of starts and number of times this value has been achieved [17]. The multi-start procedure is terminated once a target probability, typically 0.998, has been exceeded. The feasibility of the present minimization algorithm has been validated by existing solutions of global minimization reported in the literature [18].

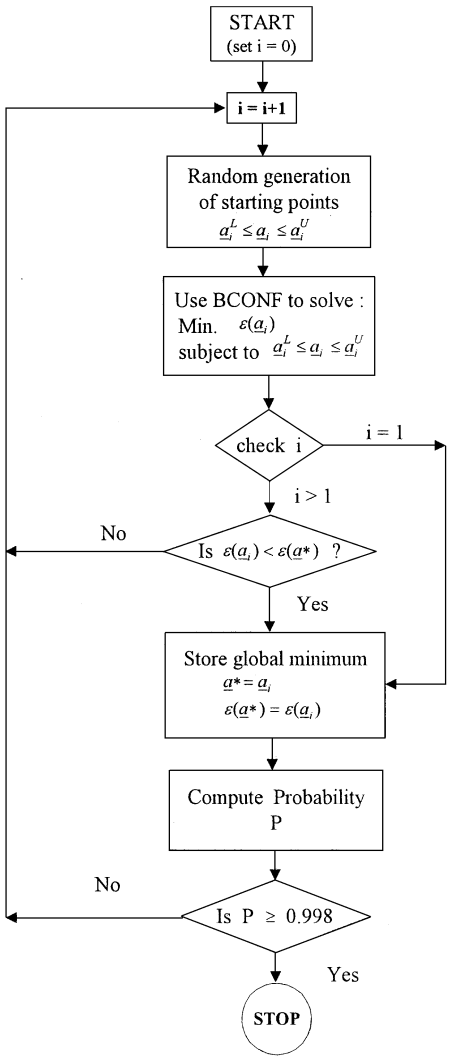

Fig. 1. Flow chart of global minimization algorithm.

EXPERIMENTAL INVESTIGATION

Two hollow shafts, A and B, made of graphite/epoxy prepreg tapes (Q-1115) supplied by the Toho Co., Japan were cured via the cure cycles as shown in Fig. 2. The dimensions of the shafts are shown in Fig. 3. It is noted that wall thicknesses of the shafts vary between the two ends of the shafts. The angles between fibers in different layers and the longitudinal axes of the shafts ranged from 0° to 10°. Shaft A was further filled with foam material and cured at room temperature. Bounds on material properties of the shafts were determined from specimens manufactured via two different curing processes as shown in Fig. 4. Curing processes A and B were used to simulate, respectively, the "best" and "worst" material properties of the shafts that might be made in factory. Curing process A is the same as the one shown in Fig. 2 and curing process B is as shown in Fig. 4. The properties of the composite materials determined from standard laboratory tests in accordance with relevant *ASTM* specifications [15] for the two curing processes are listed in Table 1 in comparison with those provided by the supplier. The densities of shafts A and B are 1450 and 726 kg/m^3, respectively. The two shafts were first subjected to static flexural tests as shown in Fig. 5. Each shaft was clamped at the end with smaller outer radius and subjected to a load of 230 gf at the other end. The shafts were mathematically divided into ten elements of equal length. Vertical displacements at nodes along the span of each shaft were measured using a displacement gage (*LVDT*). The measured displacements at nodes 5 and 10 will be used in the bending stiffness identification as described in the following

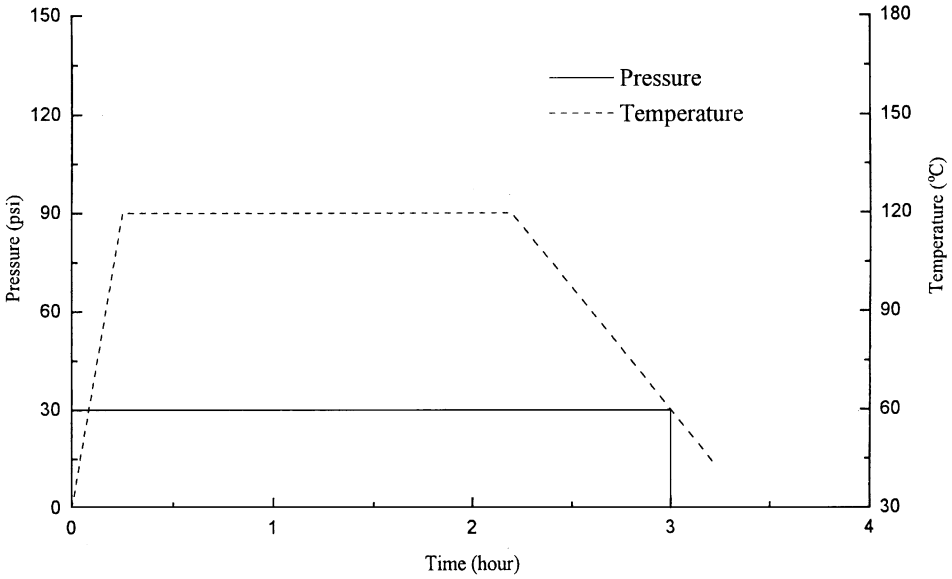

Fig. 2. Cure cycle for manufacture of laminated composite shafts.

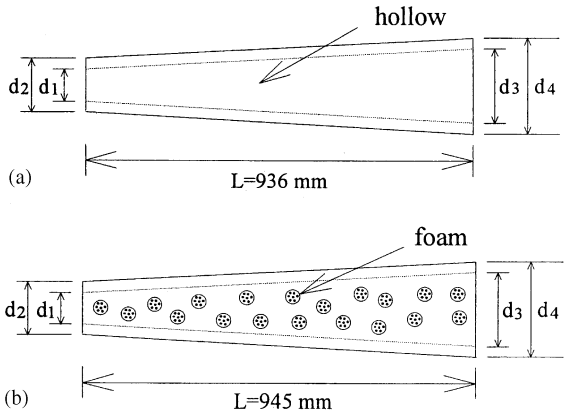

Fig. 3. Dimensions of shafts. (a) Shaft A ($d_1 = 4.48$ mm, $d_2 = 10.0$ mm, $d_3 = 15.38$ mm, $d_4 = 18.4$ mm); (b) Shaft B ($d_1 = 5.2$ mm, $d_2 = 10.05$ mm, $d_3 = 15.3$ mm, $d_4 = 18.24$ mm).

section. The two shafts were also subjected to vibration tests using a vibration measurement system which consisted of a laser vibrometer and a spectrum analyzer. The fundamental frequencies of the shafts were extracted from the measured frequency response spectrums of the shafts. Figure 6 shows the measured frequency response spectrums of shafts A and B.

DETERMINATION OF BOUNDS

The diameters of shafts A and B are assumed to vary linearly along the spans of the shafts.

$$d_i = d_1 + \frac{x}{L}(d_3 - d_1) \tag{3}$$

and

$$d_o = d_2 + \frac{x}{L}(d_4 - d_2), \tag{4}$$

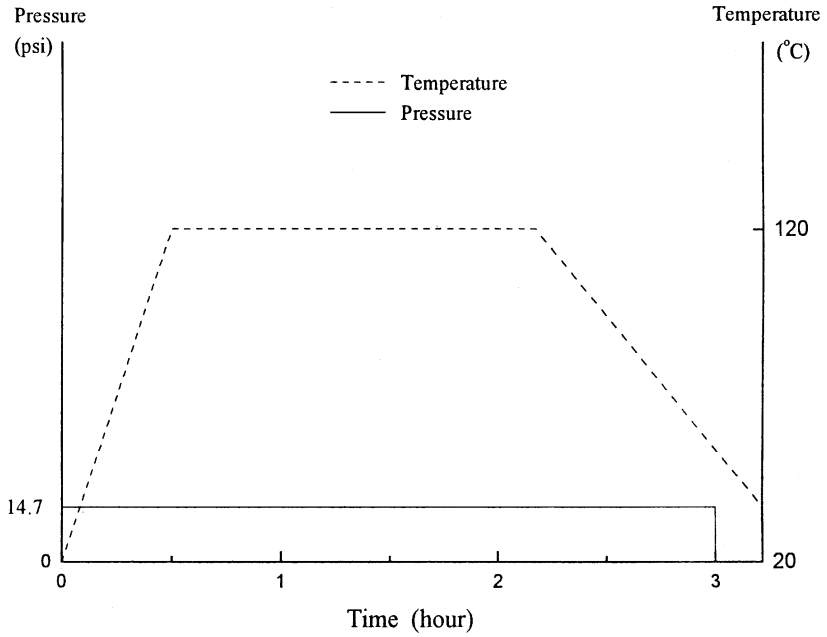

Fig. 4. Curing process B.

Table 1. Material properties of composite lamina

Cure cycle	E_1 (Gpa)	E_2 (Gpa)
A	91.0	7.2
B	80.0	6.7
Provided by Supplier	142.5	9.8

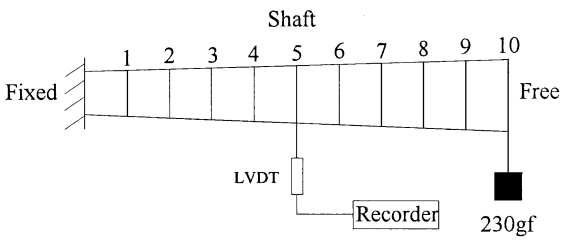

Fig. 5. Flexural test of shafts.

where d_i, d_o are the inner and outer diameters, respectively. The area moment of inertia of a hollow circular cross section is expressed as

$$I = \frac{\pi}{64}(d_o^4 - d_i^4). \tag{5}$$

The area moment of inertia at the right end of an element together with the Young's modulus E_1 obtained via curing process A are used to determine the upper bound of the bending stiffness of the element.

$$a_i^U = E_{1A} I_{iR}(1 + \eta), \quad i = 1, \ldots, m, \tag{6}$$

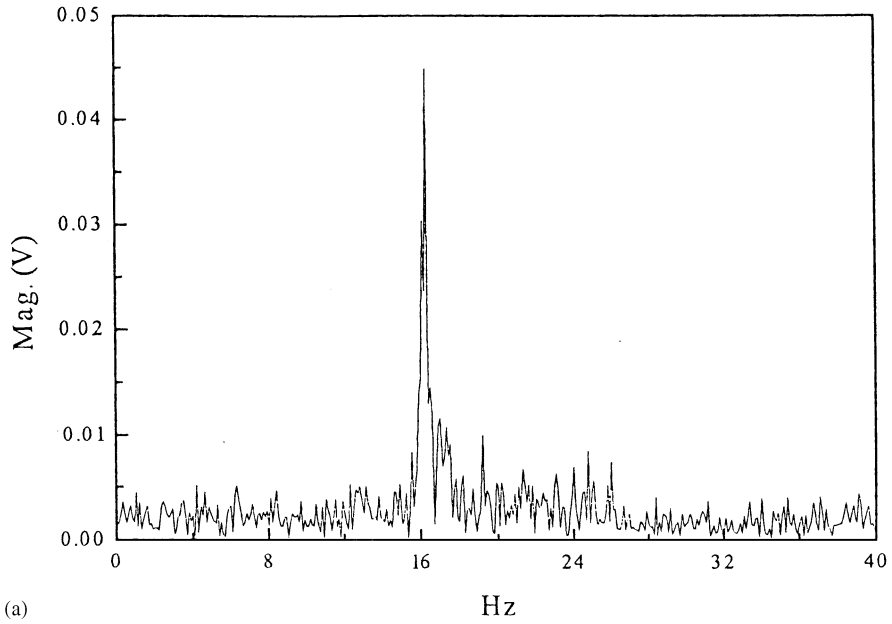

(a)

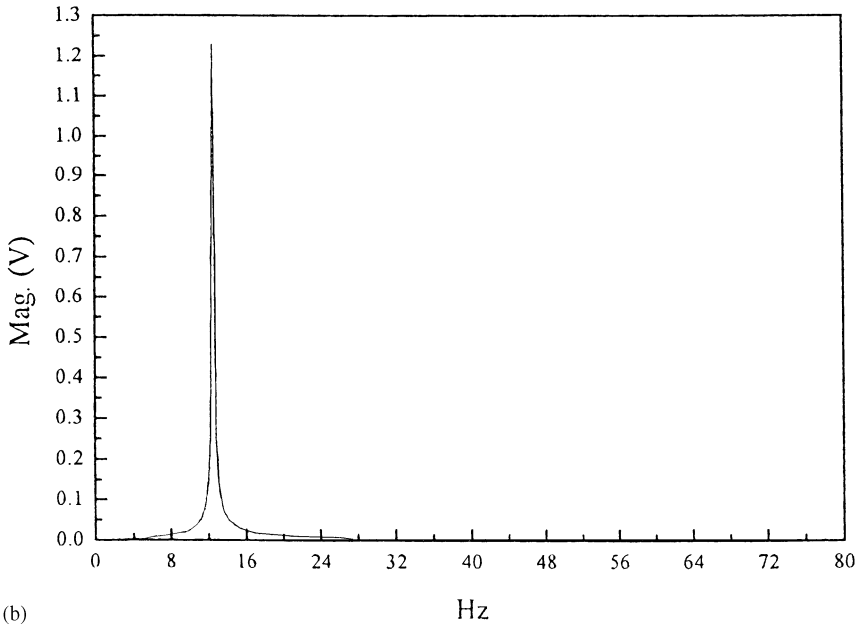

(b)

Fig. 6. Frequency response spectra of shafts. (a) Shaft A; (b) Shaft B.

where I_{iR} is the elemental bending stiffness at the right end of the ith element; E_{1A} is E_1 obtained from curing process A; η is a fraction. Similarly, the lower bounds of the elemental bending stiffnesses are expressed as

$$a_i^L = E_{1B} I_{iL}(1 - \eta), \quad i = 1, \ldots, m, \tag{7}$$

where I_{iL} is the elemental bending stiffness at the left end of the ith element; E_{1B} is E_1 obtained from curing process B.

RESULTS AND DISCUSSION

The accuracy of the present method for bending stiffness identification is first studied by means of an example. Consider the system identification of the cantilever beam which has been discretized into 10 elements of equal length as shown in Fig. 5. In the identification process, the bounds of the element bending stiffnesses in Eqn (2) are set as

$$a_i^L = a_i^*(1-\eta), \quad a_i^U = a_i^*(1+\eta).$$

The beam is subjected to a vertical force of magnitude 230 gf at the free end. The actual vertical displacements at nodes 5 and 10 are given as 2.724 and 7.434 mm, respectively. Herein, different values of η are used to identify the element bending stiffnesses of the beam. The errors of the identified element bending stiffnesses for different values of η are listed in Table 2. The actual and identified deflections of the beam are plotted in Fig. 7. It is noted that the errors of the identified deflections are insignificant. Therefore, the use of η less than or equal to 30% can give reasonably good results for the identified elemental bending stiffnesses. Next, consider the bending stiffness

Table 2. Errors of identified element bending stiffnesses using different values of η

Element No.	Actual EI ($N \cdot m^2$)	Error $= \frac{\text{Identified} - \text{Actual}}{\text{Actual}} \times 100\%$			
		$\eta = 5\%$	$\eta = 15\%$	$\eta = 25\%$	$\eta = 30\%$
1	52.1	−0.54	−2.83	−5.27	3.49
2	67.4	0.69	2.66	5.28	−9.98
3	84.7	0.68	5.61	9.68	7.05
4	104.0	−0.05	−2.13	−7.25	−5.47
5	125.0	−0.28	−3.12	−4.22	−6.81
6	147.2	−0.31	−1.88	−2.08	8.80
7	170.3	−1.19	−3.03	−5.03	5.86
8	193.7	−0.64	−1.48	−0.90	10.58
9	216.8	−0.05	0.37	−2.13	−6.92
10	238.9	0.47	1.42	5.22	8.98

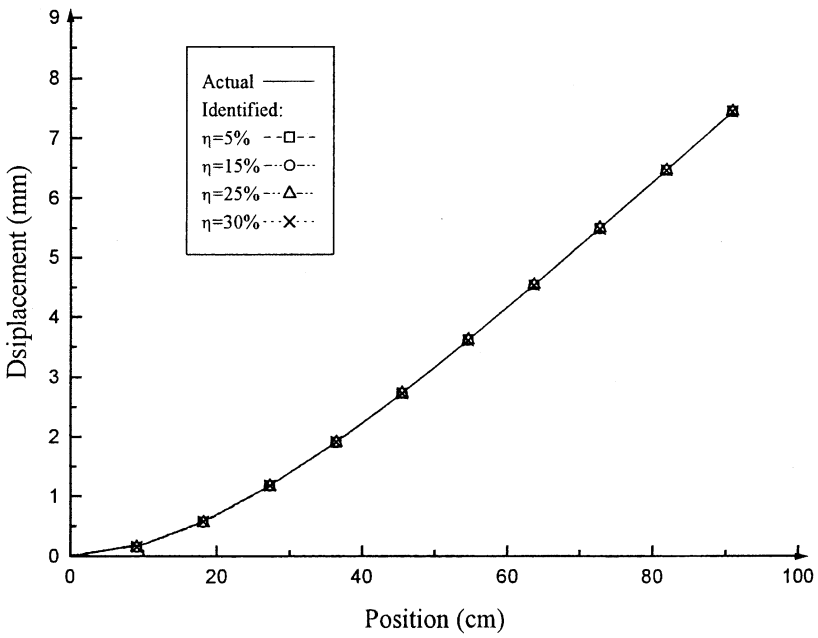

Fig. 7. Actual and identified deflections of a cantilever beam.

identification of the two shafts in Fig. 3. The shafts are discretized into 10 elements in the finite element analysis. Measured displacements at nodes 5 and 10 are used for bending stiffness identification. The bounds of the elemental bending stiffnesses are determined from Eqns (6) and (7) with the choice of $\eta = 0.1$. Using the material properties in Table 1 and the shafts dimensions in Fig. 3, the upper and lower bounds of the elemental bending stiffnesses for shafts A and B are computed and listed in Table 3. Using the proposed minimization algorithm, the identified elemental bending stiffnesses are determined and listed in Table 4. It is noted that around 10 starting points were generated and less than 10 iterations were performed for each starting point for the cases under consideration. The theoretical and experimental deflections of the shafts are listed in Table 5 for comparison. It is noted that when compared with the experimental deflections, the use of the identified elemental bending stiffnesses in the finite element analysis can yield very good results for deflection. For the comparison purpose, the elemental bending stiffnesses derived from the material properties provided by the supplier are also used in the deflection analysis of the shafts and the predicted deflections of the shafts are shown in Fig. 8. It is noted that erroneous results may be obtained if incorrect bending stiffnesses or wrong material properties are used in the analysis. It is also worth noting that if the upper or lower bounds are not properly chosen or they significantly deviate from the "exact" values, erroneous results may be obtained. For instance, if the side constraints, $0 < a_i^* < a_i^U$ $(i = 1, \ldots, m)$, are adopted for solving the minimization problem, multiple global optima will occur and incorrect elemental bending stiffnesses will be obtained even though

Table 3. Bounds of elemental bending stiffness

	Bending stiffness ($N \cdot m^2$)	
Element No	Lower bound	Upper bound
1	34	63
2	45	82
3	59	103
4	74	127
5	91	152
6	109	179
7	128	207
8	148	235
9	168	262
10	188	288

Table 4. Identified elemental bending stiffnesses

	Element bending stiffness ($N \cdot m^2$)									
Shaft	1	2	3	4	5	6	7	8	9	10
A	48.590	55.210	57.460	79.050	101.33	103.09	154.70	231.48	234.11	262.97
B	46.72	52.51	56.75	60.73	65.18	69.60	128.40	253.16	264.67	272.40

Table 5. Theoretical and experimental deflections of shafts

		Node displacement (mm)									
Shaft	Method	1	2	3	4	5	6	7	8	9	10
A	Theoretical	0.169	0.634	1.340	2.227	3.230	4.315	5.456	6.625	7.180	9.0
	Experimental	0.172	0.672	1.417	2.239	3.229	4.307	5.410	6.504	7.430	9.0
B	Theoretical	0.176	0.661	1.396	2.334	3.434	4.660	5.964	7.298	8.646	10.0
	Experimental	0.160	0.623	1.374	2.122	3.434	4.559	5.847	7.014	8.146	10.0

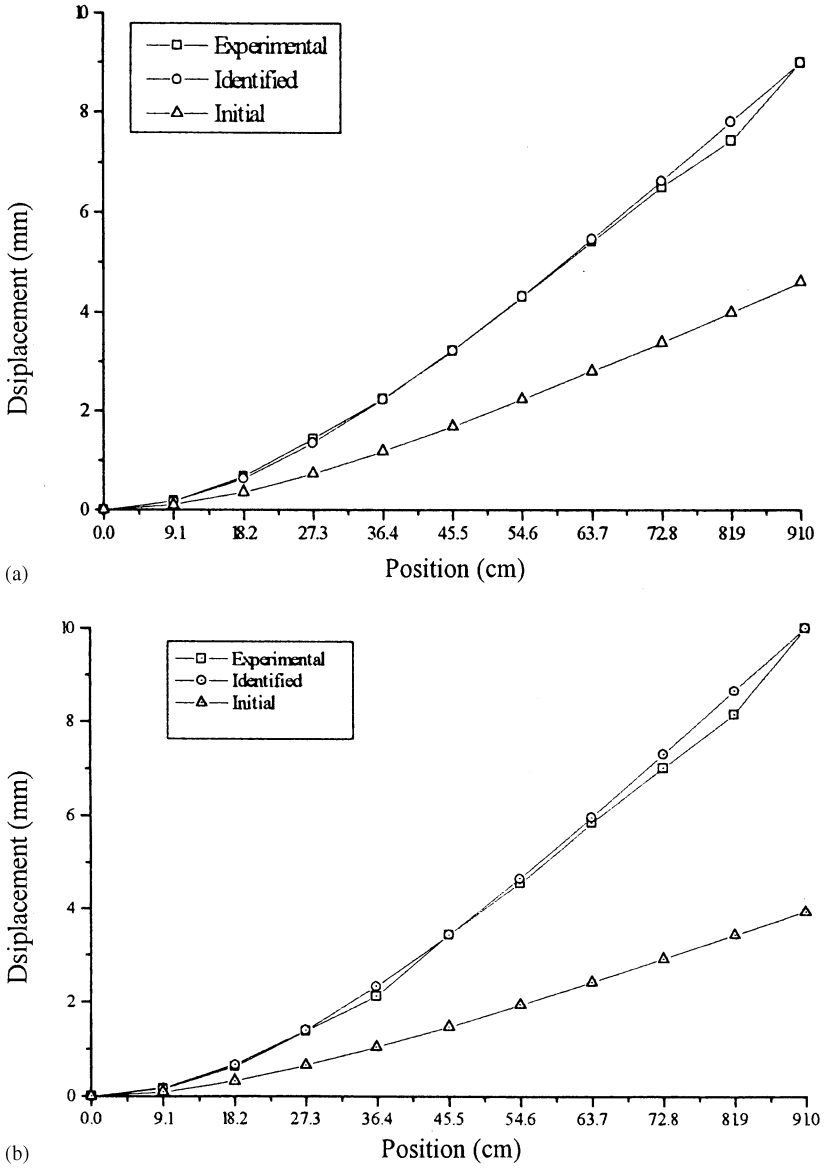

Fig. 8. Deflections of shafts obtained by different methods. (a) Shaft A; (b) Shaft B.

the theoretically predicted displacements at the two measured points agree well with the experimental ones. Therefore, the choice of proper bounds for the elemental bending stiffnesses is vital for having a successful parameter identification. It is noted that since the differences between the material properties obtained from cure cycles A and B are small, the process of determining bounds of elemental bending stiffnesses can be further simplified by using the material properties obtained from cure cycle A together with an appropriate value of η. In general, good engineering judgement and experience can help make an appropriate choice. Next, consider the capability of the identified parameters in determining the fundamental frequencies of the shafts. It has been found that theoretically determined fundamental frequencies can closely match the experimental results as shown in Table 6.

CONCLUSIONS

The bending stiffness identification of laminated composite shafts was studied using a global minimization algorithm. Bounds on design variables were determined from experimental results.

Table 6. Theoretical and experimental fundamental frequencies

Shaft	Fundamental frequency (Hz)		Error $\left\lvert\frac{\text{I} - \text{II}}{\text{II}}\right\rvert$ %
	Theoretical (I)	Experimental (II)	
A	15.1	16.3	7.4
B	12.4	12.6	1.6

Flexural tests of the shafts were performed and displacements at two points on each shaft were used for the bending stiffness identification. It was found that the proposed minimization algorithm when used with proper choice of bounds on elemental bending stiffnesses could yield reasonably good results for the identified elemental bending stiffnesses. Vibration test data were also used to further validate the proposed method. The proposed method may find applications for material characterization or damage detection of different types of laminated composite members such as golf shafts, rotor shafts, transmission shafts and pipes.

Acknowledgement—This research work was supported by the National Science Council of the Republic of China under Grant No. NSC 85-2212-E009-019. Their support is gratefully appreciated.

REFERENCES

1. Lubin, G., *Handbook of Composites*. van Nostrand Reinhold Co, London, 1982.
2. Schwartz, M. M., *Composite Materials Handbook*. McGraw-Hill, New York, 1983.
3. Salkind, M. J., Fatigue of composites, composite materials: testing and design (2nd Conference). *ASTM STP* 497, 1972, pp. 143–169.
4. Crema, L. B., Castellani, A. and Coppotelli, G., Damage localization in composite material structures by using eigenvalue measurements. *ASME, Materials and Design Technology*, 1995, PD-**71**, 201–205.
5. Bar-Cohen, Y., NDE of fiber reinforced composites: a review. *Materials Evaluation*, 1986, **44**, 446–454.
6. Erdmann-Jesnitzer, F. and Winkler, T., Application of the holographic nondestructive testing method for evaluation of disbonding in sandwich plates. *Advances in Composite Materials*, 1980, ICCM3, (2), 1029–1039.
7. Wells, D. R., NDT of sandwich structures by holographic interferometry. *Materials Evaluation*, 1969, **27**, 225–226.
8. Berman, A. and Nagy, E. J., Improvement of a large analytical model using test data. *AIAA J*., 1983, **21**, 1168–1173.
9. Kam, T. Y. and Lee, T. Y., Crack size identification using an expanded mode method. *International Journal of Solids and Structures*, 1994, **31**, 925–940.
10. Kam, T. Y. and Lee, T. Y., Detection of cracks in structures using model test data. *Engineering Fracture Mechanics*, 1992, **42**, 381–387.
11. Lee, T. Y. and Kam, T. Y., A global minimization method for crack location identification. *Journal of Engineering Optimization*, **21**, 147–159.
12. Wei, F. S., Mass and stiffness interaction effects in analytical model modification. *AIAA J*., 1990, **28**, 1686–1688.
13. Farhat, C. and Hemez, F. M., 1993, Updating finite element dynamic models using an element-by-element sensitivity methodology, *AIAA J*., 1993, **31**, 1702–1711.
14. Gallagher, R. H., *Finite Element Analysis: Fundamentals*. Prentice-Hall, N.J., 1975.
15. ASTM Standard and Literature References for Composite Material, 2nd ed. 1990.
16. IMSL *user's Manual*, Houston, U.S.A., 1989.
17. Synman, J. A. and Fatti, L. P., A multi-start global minimization algorithm with dynamic search trajectories, *Journal of Optimum Theory and Applications*, 1987, **54**, 121–141.
18. Ballard, D. H., Jelinek, C. A. and Schinzinger, R., An algorithm for the solution of constrained generalized polynomial programming problems. *Computer Journal*, 1974, **17**, 261–266.